

Evidence against naive truncations of the OPE from $e^+e^- \rightarrow$ hadrons below charm

Diogo Boito,^a Maarten Golterman,^b Kim Maltman,^{c,d} Santiago Peris^e

^a*Instituto de Física de São Carlos, Universidade de São Paulo
CP 369, 13570-970, São Carlos, SP, Brazil*

^b*Department of Physics and Astronomy, San Francisco State University
San Francisco, CA 94132, USA*

^c*Department of Mathematics and Statistics, York University
Toronto, ON Canada M3J 1P3*

^d*CSSM, University of Adelaide, Adelaide, SA 5005 Australia*

^e*Department of Physics and IFAE-BIST, Universitat Autònoma de Barcelona
E-08193 Bellaterra, Barcelona, Spain*

The operator product expansion (OPE), truncated in dimension, is employed in many contexts. An example is the extraction of the strong coupling, α_s , from hadronic τ -decay data, using a variety of analysis methods based on finite-energy sum rules. Here, we reconsider a long-used method, which parametrizes non-perturbative contributions to the $I = 1$ vector and axial vacuum polarizations with the OPE, setting several higher-dimension coefficients to zero in order to implement the method in practice. The assumption that doing this has a negligible effect on the value of α_s is tantamount to the assumption that the low-dimension part of the OPE converges rapidly with increasing dimension near the τ mass. Were this assumption valid, it would certainly have to be valid at energies above the τ mass as well. It follows that the method can be tested using data obtained from $e^+e^- \rightarrow$ hadrons, as they are not limited by the kinematic constraints of τ decays. We carry out such an investigation using a recent high-precision compilation for the R -ratio, arguing that it provides insights into the validity of the strategy, even if it probes a different, though related channel. We find that e^+e^- -based tests call into question the implied assumption of rapid convergence of the low-dimension part of the OPE around the τ mass, and thus underscore the need to restrict finite-energy sum-rule analyses to observables which receive only contributions from lower-order terms in the OPE.

I. INTRODUCTION

As is well known, the spectral function, $\rho_{\text{EM}}(s)$, of Π_{EM} , the scalar polarization of the electromagnetic (EM) current-current two-point function, is directly obtainable from the experimentally measured R -ratio,

$$R(s) \equiv \frac{3s}{4\pi\alpha^2} \sigma_{e^+e^- \rightarrow \text{hadrons}(\gamma)}(s) = \frac{\sigma_{e^+e^- \rightarrow \text{hadrons}(\gamma)}(s)}{\sigma_{e^+e^- \rightarrow \mu^+\mu^-}(s)}, \quad (1.1)$$

via

$$\rho_{\text{EM}}(s) = \frac{1}{\pi} \text{Im} \Pi_{\text{EM}}(s) = \frac{1}{12\pi^2} R(s), \quad (1.2)$$

where, in Eq. (1.1), α is the fine-structure constant, the second of the equations holds for values of s for which the muon mass can be neglected, and the γ in parentheses indicates that the hadronic states in question are inclusive of final-state radiation.

Similarly, information on the spectral functions, $\rho_{V/A;ij}^{(J)}(s)$, of the spin $J = 0, 1$ scalar polarizations, $\Pi_{ij;V/A}^{(J)}$, of the flavor $ij = ud$ and us vector (V) and axial vector (A) current-current two-point functions can be obtained from the experimental hadronic τ -decay distributions, $dR_{V/A;ij}/ds$. Explicitly [1],

$$\frac{dR_{V/A;ij}(s; s_0)}{ds} = \frac{12\pi^2 |V_{ij}|^2 S_{\text{EW}}}{s_0} \left[w_\tau(y_\tau) \rho_{V/A;ij}^{(0+1)}(s) - w_L(y_\tau) \rho_{V/A;ij}^{(0)}(s) \right], \quad (1.3)$$

where $y_\tau = s/m_\tau^2$,

$$\begin{aligned} w_\tau(y) &= (1-y)^2(1+2y), \\ w_L(y) &= 2y(1-y)^2, \end{aligned} \quad (1.4)$$

S_{EW} is a known short-distance electroweak correction [2], V_{ij} is the flavor ij CKM matrix element¹ and $dR_{V/A;ij}(s; s_0)/ds$ is related to the total inclusive hadronic τ -decay width by

$$\begin{aligned} R_{V/A;ij}(s_0) &= \int_0^{s_0} ds \frac{dR_{V/A;ij}(s; s_0)}{ds}, \\ R_{V/A;ij}(m_\tau^2) &= \frac{\Gamma[\tau^- \rightarrow \nu_\tau \text{ hadrons}_{V/A;ij}(\gamma)]}{\Gamma[\tau^- \rightarrow \nu_\tau e^- \bar{\nu}_e(\gamma)]}. \end{aligned} \quad (1.5)$$

The analyticity properties of current-current polarizations (denoted generically by Π) ensure the validity of finite-energy sum rules (FESRs), which allow one to relate weighted integrals over the associated experimental spectral data to theoretical representations of the polarizations [3]. Explicitly, for any $\Pi(s)$ free of kinematic singularities, any $s_0 > 0$, and any $w(s)$ analytic inside and on the contour $|s| = s_0$, one has the sum rule

$$I_w^{\text{exp}}(s_0) = I_w^{\text{th}}(s_0), \quad (1.6)$$

¹ Eq. (1.3) has been written in terms of spectral function combinations, $\rho_{V/A;ij}^{(0+1)}(s)$ and $s\rho_{V/A;ij}^{(0)}$, for which the corresponding polarizations, $\Pi_{V/A;ij}^{(0+1)}(s)$ and $s\Pi_{V/A;ij}^{(0)}(s)$, are free of kinematic singularities.

where the weighted integrals over the experimental spectral function and over the vacuum polarization are defined as

$$I_w^{\text{exp}}(s_0) = \frac{1}{s_0} \int_0^{s_0} ds w\left(\frac{s}{s_0}\right) \rho(s) , \quad (1.7a)$$

$$I_w^{\text{th}}(s_0) = -\frac{1}{2\pi i s_0} \oint_{|s|=s_0} ds w\left(\frac{s}{s_0}\right) \Pi(s) . \quad (1.7b)$$

For sufficiently large s_0 , $I_w^{\text{th}}(s_0)$ can be approximated using the operator product expansion (OPE) for Π . This allows quantities entering the OPE (such as the strong coupling α_s , quark masses, and effective higher-dimension vacuum condensates) to be related to experimental data, in principle. FESRs based on $ud - us$ flavor-breaking differences of hadronic τ -decay distributions can also be used to provide an independent determination of $|V_{us}|$ [4–6]. Generalizing Eq. (1.6) to weights $w(s)/s^N$, still with $w(s)$ analytic, yields analogous inverse-moment FESR (IMFESR) relations involving quantities such as $\Pi(0)$, and its derivatives with respect to s at $s = 0$, which can be exploited to determine some of the low-energy constants of chiral perturbation theory (ChPT), provided those terms in the associated OPE required for the $w(s)$ chosen are known from external sources [7]. The OPE thus plays an important role in FESR and IMFESR analyses.

Information on the flavor ud , us V and A spectral functions from hadronic τ -decay data is, of course, only available up to the kinematic limit, $s = m_\tau^2$, restricting FESRs and IMFESRs based on hadronic τ -decay data to $s_0 \leq m_\tau^2$. No such kinematic limit exists for FESRs and IMFESRs based on hadronic electroproduction cross-section data.

The OPE is expected to provide an accurate representation of $\Pi(s)$ valid for Euclidean $Q^2 \equiv -s \gg \Lambda_{\text{QCD}}^2$, up to small exponentially suppressed corrections. In Eq. (1.7b), the OPE representation, however, must be used over the whole of the contour $|s| = s_0$, which includes the region near the Minkowski axis, where, as anticipated in Ref. [8], the OPE breaks down at intermediate (timelike) s . This is clear from the presence of resonance peaks in experimental spectral functions at s of order a few GeV^2 . Such “duality violating” (DV) effects are expected to be localized to the vicinity of the Minkowski axis, an expectation confirmed by studies of FESRs employing both “unpinched” weights (those which do not vanish at $s = s_0$ and hence do not suppress contributions from the region near the Minkowski axis) and “pinched” weights (those with $w(s_0) = 0$, which do suppress contributions from that region) [9]. Precision determinations of α_s , quark masses, and other OPE parameters may, however, require small residual DV contributions to be taken into account, even for FESRs involving pinched weights [10, 11].

A second, related issue for the use of the OPE in FESRs and IMFESRs is the fact that the OPE (an expansion in $z = 1/Q^2$) is not convergent [12]. Convergence would require the existence of a region in the complex plane around $z = 0$ free of singularities, and hence, in the case of a current-current two-point function, the vanishing of the corresponding spectral function above some maximum value of s . This is not the case. The OPE is thus, at best, an asymptotic expansion, and one cannot safely assume that effective condensates C_D , of

dimension D , defined by²

$$\Pi_{\text{OPE}}(-Q^2) = \sum_{k=0}^{\infty} \frac{C_{2k}(Q^2)}{(-Q^2)^k}, \quad (1.8)$$

naively scale as Λ_{QCD}^D .

This is relevant for FESRs and IMFESRs employing weights $w(s)$ which generate OPE contributions proportional to higher dimension C_D not known from external sources. Assumptions based on naive scaling of the C_D have often been used to argue that such unknown contributions are “safely” negligible at scales of a few GeV^2 , including $s_0 \sim m_\tau^2$. In general, a polynomial weight $w(y) = \sum_{k=0}^N b_k y^k$, $y = s/s_0$, produces, up to logarithmic corrections suppressed by additional powers of α_s , a contribution

$$\sum_k (-1)^k b_k C_{2k+2}/s_0^{k+1} \quad (1.9)$$

to the right-hand side of Eq. (1.6).

We refer to the prescription of neglecting contributions proportional to $b_k C_{2k+2}$ for higher k and s_0 of order a few GeV^2 as the “truncated OPE” (tOPE) approach [13]. The non-convergence of the OPE implies that this assumption is a dangerous one to make, in general. It does, however, remain a logical possibility that, for a given value of s_0 , the truncated OPE might represent a reasonable approximation for a specific set of weights. If so, the tOPE approach can be used for a sum-rule analysis employing this set of weights at this value of s_0 . In this paper, we will investigate whether or not this is the case for the EM current-current two-point function for values of s_0 between m_τ^2 and 4 GeV^2 .

An example of a situation in which the tOPE approximation might be practically useful is provided by the FESR determination of α_s based on non-strange hadronic τ decay data. Since the kinematic weight $w_\tau(y) = 1 - 3y^2 + 2y^3$ appearing in Eq. (1.3) has degree 3, the OPE representation of the total non-strange hadronic τ -decay width contains contributions of dimension 0, 6 and 8.³ The total non-strange width (corresponding to the kinematically weighted spectral integral with $s_0 = m_\tau^2$) is thus insufficient, by itself, to allow one to determine α_s since the relevant condensates, C_6 and C_8 are not known from external sources. A tOPE strategy to deal with this problem, proposed in Ref. [15], is to consider additional FESRs in which C_6 and C_8 also occur. The conventional version of this strategy employs the five “ $k\ell$ spectral weights,”

$$w_{k\ell}(y) = (1 + 2y)(1 - y)^{2+k} y^\ell, \quad (1.10)$$

with $k\ell = 00, 10, 11, 12$ and 13 (note that $w_{00} = w_\tau$), and focuses on the $s_0 = m_\tau^2$ versions of the corresponding spectral integrals (1.7a). Recent versions of this analysis may be found in Refs. [16, 17]. A number of alternate weight sets, including the so-called “optimal weights,”

$$w_{2k}(y) = 1 - (k + 2)y^{k+1} + (k + 1)y^{k+2}, \quad (1.11)$$

² The condensates are logarithmically dependent on Q^2 . This dependence, which is suppressed by at least one power of α_s , is usually neglected for $D \geq 4$, as it makes no difference in the value of α_s obtained from FESR analyses [11].

³ $D = 4$ contributions are strongly suppressed by the absence of a term linear in y in $w_\tau(y)$. For the case of non-strange τ decays, C_2 is proportional to the square of the light quark mass, and is numerically negligible. For the case of the R -ratio, there is a contribution proportional to the square of the strange quark mass which can be calculated; for details we refer to Ref. [14].

$k = 1, \dots, 5$, were also considered in Ref. [17] (note that $w_{21} = w_\tau$),⁴ with s_0 again restricted to m_τ^2 .⁵

The tOPE assumption enters these analyses as follows. Since both the $k\ell$ spectral and optimal weight sets involve weights with degrees up to 7, OPE contributions up to $D = 16$ are in principle required, as per Eq. (1.9). So long as one attempts to minimize residual DV contributions by restricting s_0 to its maximum kinematically allowed value, m_τ^2 , a five-weight set provides only five (highly correlated) spectral integrals for use in fitting, and one can hence fit at most four OPE parameters. The five $k\ell$ spectral weight FESRs, however, in general, involve OPE contributions depending on α_s , and the seven condensates C_4, \dots, C_{16} . The five optimal-weight FESRs, similarly, neglecting the strongly suppressed $D = 4$ contributions, depend on the OPE parameters α_s and C_6, \dots, C_{16} . In both cases, the number of OPE parameters exceeds the number of $s_0 = m_\tau^2$ spectral integrals, unless one makes the tOPE assumption, which is to neglect contributions from the new C_D introduced by the higher degree weights. In the tOPE implementation of the conventional $k\ell$ spectral-weight analysis, contributions proportional to C_{10}, C_{12}, C_{14} and C_{16} are assumed negligible, leaving the four remaining OPE parameters α_s, C_4, C_6 and C_8 to be fit. In the tOPE implementation of the optimal-weight analysis, contributions proportional to C_{12}, C_{14} and C_{16} are assumed negligible and the five spectral integrals are used to fit the four remaining relevant OPE parameters, α_s, C_6, C_8 and C_{10} . In both cases, the assumption underlying the tOPE approach is that the OPE, though not actually convergent, nonetheless behaves, for $s_0 = m_\tau^2$, as if it were a rapidly converging series out to at least $D = 16$.

Since both integrated DV contributions and integrated higher-dimension OPE contributions decrease with increasing s_0 , it follows that, if the tOPE assumption is reliable at $s_0 = m_\tau^2$, it should be even more reliable for $s_0 > m_\tau^2$. Unfortunately, the kinematic restriction $s_0 \leq m_\tau^2$ prevents the self-consistency tests this suggests from being carried out for τ -based FESRs. Analogous tests can, however, be carried out for FESRs based on EM R -ratio data, where there is no kinematic restriction on the hadronic invariant mass-squared s .⁶

As already mentioned, the aim of this paper is to investigate the validity of the tOPE strategy using data for the EM spectral function obtained from $e^+e^- \rightarrow \text{hadrons}(\gamma)$. This is not an exercise of academic interest since, as was shown in Ref. [13], the assumptions underpinning the tOPE strategy affect the value extracted for α_s using this strategy. We will use the recent compilation of exclusive experimental data for the R -ratio provided in Ref. [18], which was also recently employed in a determination of α_s using a different strategy [14]. The sum-of-exclusive-modes part of the compilation of Ref. [18] reaches up to $s = 4 \text{ GeV}^2$, after which the compilation relies on inclusive data sets. We show these data in Fig. 1 in the region $2 \text{ GeV}^2 \leq s \leq 6 \text{ GeV}^2$, with the transition from exclusive to inclusive regions clearly visible. In Ref. [14] it was found that including the much more scarce data above $s = 4 \text{ GeV}^2$ leads to values of α_s consistent with those found from the exclusive data, but without decreasing the error. Also, using Eq. (1.6) with only values of s_0 in the inclusive region leads to a still consistent, but higher value of α_s with a much larger error.

⁴ The absence of a term linear in y again strongly suppresses $D = 4$ OPE contributions for the optimal weight FESRs.

⁵ In Ref. [17], s_0 dependence was considered, but all final values quoted for $\alpha_s(m_\tau^2)$ were obtained from moments at $s_0 = m_\tau^2$.

⁶ For other tests of the tOPE strategy, based on the hadronic τ -decay data, see Ref. [13].

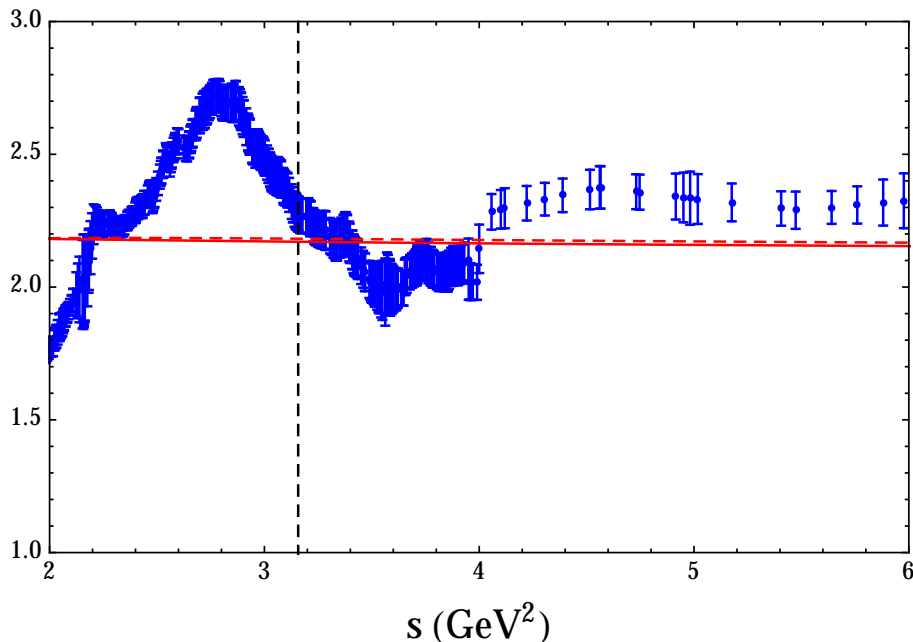


FIG. 1: A blow-up of R -ratio in the region $2 \leq s \leq 6 \text{ GeV}^2$ [18]. The red solid and red dashed lines show the results obtained from perturbation theory with $\alpha_s(m_\tau^2) = 0.28$ and $\alpha_s(m_\tau^2) = 0.32$, respectively. The vertical dashed line is $s = m_\tau^2$.

The reason is that the inclusive data for the R -ratio tends to be larger than what one would expect from perturbation theory, *cf.* the red solid and dashed curves in Fig. 1. However, despite the visually apparent tension between the inclusive data and perturbation theory, it was found that the larger values of these data are consistent with it being a statistical fluctuation, given the strong correlations that exist between the inclusive data points at different values of s .

Given all this, we will limit ourselves in this paper to an investigation of the tOPE approach using the R -ratio data up to $s = 4 \text{ GeV}^2$; this is the same region employed in the determination of α_s in Ref. [14].

The rest of this paper is organized as follows. Having already reviewed the tOPE strategy and the goal of this paper in this section, we discuss in more detail the assumptions on which our investigation will rely, and elaborate further on our methodology, in Sec. II. Then, in Sec. III, we will present our results, which are shown in Figs. 3 to 10, and explained in the main text. A final section restates our assumptions and contains our conclusions. A preliminary account of this work was presented in Ref. [19].

II. ASSUMPTIONS AND METHODOLOGY

The tOPE strategy has often been employed previously in analyses of FESRs based on hadronic τ -decay data. As our aim is to use values of s_0 greater than m_τ^2 to test the strategy, we will focus instead on FESRs based on EM spectral data. The spectral function obtained

from the R -ratio is, of course, not the same as the spectral functions obtained from τ decays. Here, we discuss the differences in some detail, spelling out the assumptions underlying our use of analyses based on the former to cast light on those based on the latter.

It has been advocated, in the literature applying the tOPE strategy to τ -decay data, that analyses of the sum $V + A$ of the non-strange V and A channels are preferable, based on the notion that this sum will be less sensitive to duality violations, and that, in general, non-perturbative effects may be smaller for the sum than for the individual V or A channels. Of course, in the EM case only a V -channel spectral function is available, as the photon does not couple to axial currents. There are two reasons to believe that, nevertheless, it is reasonable to expect that useful lessons can be learned by considering the purely V -channel EM current only.

First, it was found in Ref. [14] that for a determination of α_s from R -ratio data in the region above about 3.25 GeV^2 duality violations can be neglected, with results that are fully consistent with a sum-rule analysis of the τ -based spectral data which modeled duality violations below the τ mass. This observation implies that the OPE should provide a good representation of the contour integral over $\Pi(s)$ in Eq. (1.7b) if the radius s_0 is chosen to be not smaller than approximately 3.25 GeV^2 . As we will draw our main conclusions from fits of electroproduction data with values of s_0 above the τ mass, it therefore appears that the issue of sensitivity to duality violations does not constitute a problem for tests of the tOPE strategy based on EM V -channel data.

Moreover, the tOPE-based results obtained in Ref. [17] show excellent consistency for the values of α_s extracted from V -channel fits and $V + A$ -channel fits, employing the weights of Eqs. (1.10) and (1.11). The values obtained from $k\ell$ spectral weights differ by slightly more than 1σ between V and $V + A$,⁷ while those obtained from optimal weights differ by much less than 1σ . In both cases, the quality of the V -channel fits is better than that of the $V + A$ channel fits, as measured by the χ^2 value per degree of freedom.

Therefore, while we have to assume that V -channel-only investigations can shed light on the tOPE strategy as applied to τ decays, it appears to us that this is, in fact, a rather innocuous assumption.

A second difference between a τ -based analysis and an R -ratio-based analysis is that the non-strange spectral functions obtained from τ decays have isospin $I = 1$, while the spectral function obtained from the R -ratio has both $I = 1$ and $I = 0$ components.⁸ We thus need to assume that the OPE behavior of the scalar polarization Π_{EM} is similar to that of the scalar polarization $\Pi_{I=1}$, if we want to use R -ratio based tests to investigate the validity of the tOPE strategy as applied to analyses of hadronic τ -decay data.

In this paper, we will make this assumption, believing that it is well motivated. If the strange-quark mass m_s were to be negligibly small, like the up- and down-quark masses, the $I = 1$ and $I = 0$ currents would be components of an $SU(3)$ -flavor multiplet, and any conclusions reached in the study of the EM polarization would directly apply to the $I = 1$ case. For $|s| = s_0$, the OPE for $\Pi_{\text{EM}}(s)$ differs from that for $\Pi_{I=1}(s)$ by terms of order m_s^2/s_0 , which for $s_0 \geq m_\tau^2$ is smaller than $m_s^2/m_\tau^2 \sim 0.003$. Indeed, in Ref. [14] it was found that the effect of m_s on the central values of $\alpha_s(m_\tau^2)$ and the OPE condensates $C_{6,8,10}$ is significantly smaller than the fit error on the values of these parameters. In addition, we

⁷ Very similar results were found in Ref. [16].

⁸ Since the up and down quark masses can be taken to vanish in a sum rule extraction of α_s , we can assume the τ -based spectral functions to be purely $I = 1$.

emphasize again that Ref. [14] finds excellent agreement between α_s determinations based on R -ratio and the τ data, if the OPE is treated consistently and the same strategy is used in both cases [11, 20, 21]. We conclude that it seems unlikely that the presence of an $I = 0$ component in the EM case would have a significant impact on the applicability of the tOPE strategy to R -ratio data, in comparison with τ -decay data, at least if the value of s_0 is large enough.

In our study of the tOPE, we will repeat the V -channel fits carried out in Ref. [17], employing the weights (1.10) and (1.11), but now using the R -ratio data compilation of Ref. [18]. We will consider values of s_0 ranging from m_τ^2 to 4 GeV^2 . If we find a good fit, we will compare the experimental spectral moments $I_w^{\text{exp}}(s_0)$ and their theoretical representation based on that fit $I_w^{\text{th}}(s_0)$ as follows. First, if we fit at the value $s_0 = s_0^*$, we compute the differences

$$\begin{aligned}\Delta_w^{\text{exp}}(s_0; s_0^*) &\equiv I_w^{\text{exp}}(s_0) - I_w^{\text{exp}}(s_0^*) , \\ \Delta_w^{\text{th}}(s_0; s_0^*) &\equiv I_w^{\text{th}}(s_0) - I_w^{\text{th}}(s_0^*) ,\end{aligned}\tag{2.1}$$

as a function of s_0 . Note that the correlations between spectral integrals at different s_0 , as well as those between OPE integrals at different s_0 , are very strong; working with the differences in Eq. (2.1) helps to avoid being misled by these correlations when comparing experimental and fitted theory integrals. Then, in order to compare experiment and theoretical representation, we compute the differences

$$\Delta_w^{(2)}(s_0; s_0^*) \equiv \Delta_w^{\text{th}}(s_0; s_0^*) - \Delta_w^{\text{exp}}(s_0; s_0^*) ,\tag{2.2}$$

where all correlations, including those between data and fit parameters, are fully taken into account. Considering these double differences avoids any issues with under- or over-estimating errors in the comparison between theory and experiment. Note that, by construction, $\Delta_w^{(2)}(s_0^*; s_0^*) = 0$, with zero uncertainty.

We will have reason to consider both fully correlated χ^2 fits and what we will refer to as “diagonal” fits, where, in the positive quadratic form to be minimized, we only retain the diagonal part of the covariance matrix for the integrated spectral data (in computing this covariance matrix, however, the full data covariance matrix is taken into account). We emphasize that, when computing errors on the fitted parameter values produced by such diagonal fits, we take into account the full covariance matrix for the integrated spectral data, without ignoring any correlations. Although correlated fits are more popular, such diagonal fits can also be a useful tool in cases where the strong correlations make a correlated fit fail. For a detailed explanation of the diagonal fit procedure, we refer the reader to the appendix of Ref. [11]. All correlations, including those between data and fit parameters, are always fully taken into account in the computation of the single and double differences $\Delta_w^{\text{exp/th}}(s_0; s_0^*)$ and $\Delta_w^{(2)}(s_0; s_0^*)$, for both types of fits.

III. RESULTS

We begin with showing and discussing some numerical results from fits employing the tOPE strategy, using fixed-order perturbation theory (FOPT).⁹ In Table 1 we show tOPE

⁹ Results from contour-improved perturbation theory (CIPT) [22] are very similar, and we will thus restrict ourselves to FOPT, for simplicity. For detailed studies comparing FOPT with CIPT, see Refs. [23, 24].

s_0^* (GeV ²)	χ^2/dof	p -value	$\alpha_s(m_\tau^2)$	$\alpha_s(m_\tau^2)$ (diag)
m_τ^2	62.7/1	2×10^{-15}	0.308(4)	0.245(10)
3.6	0.669/1	0.41	0.264(5)	0.256(12)

TABLE 1: *Fit results with optimal weights. We show the fits at $s_0^* = m_\tau^2$ and at a value of s_0^* for which the fit has a p -value greater than 10%. Errors shown are fit errors only.*

s_0^* (GeV ²)	χ^2/dof	p -value	$\alpha_s(m_\tau^2)$	$\alpha_s(m_\tau^2)$ (diag)
m_τ^2	87.8/1	7×10^{-21}	0.322(3)	0.281(6)
3.7	1.97/1	0.16	0.277(5)	0.268(9)

TABLE 2: *Fit results with $k\ell$ spectral weights. We show the fits at $s_0^* = m_\tau^2$ and at a value of s_0^* for which the fit has a p -value greater than 10%. Errors shown are fit errors only.*

fit results with optimal weights. We first attempted a correlated fit at $s_0^* = m_\tau^2$, precisely following the strategy of Ref. [17], but employing R -ratio data instead of hadronic τ -decay data. We find, as the table shows in the first line, that this fit is very bad. To the right of the double vertical line, we show the corresponding value of $\alpha_s(m_\tau^2)$ obtained from a diagonal fit. Not surprisingly, the fit values of $\alpha_s(m_\tau^2)$ for these two fits do not agree. We observe that, while the correlated fit produces what, nominally at least, looks like a reasonable result for $\alpha_s(m_\tau^2)$, this result cannot be accepted because of the very bad fit quality. The value of $\alpha_s(m_\tau^2)$ from the diagonal fit, on the other hand, is very low in comparison with the world average, $\alpha_s(m_\tau^2) = 0.315(9)$ [25, 26].

We repeated the same exercise employing $k\ell$ spectral weights, with the results shown in the first line of Table 2. The results look qualitatively similar to those shown in Table 1, but they are not in quantitative agreement.

Clearly, our attempts to apply the tOPE strategy of Ref. [17] at $s_0^* = m_\tau^2$ to the electro-production data lead to disastrous results, and an obvious question is what causes this to happen. Assuming that there is no problem with the data (which have been extensively used in Refs. [14, 18]) leads to the conclusion that the tOPE strategy does not provide a good fit of the R -ratio data, while, according to Refs. [16, 17], it does provide a good fit of the τ -decay data.¹⁰ In fact, it was already observed in Ref. [14] that the OPE does not give a good representation of the w_τ -spectral integral of the R -ratio data for $s_0 \lesssim 3.25 \text{ GeV}^2$ even when no terms from the OPE selected by Eq. (1.9) were neglected in the analysis. Since consistently good fits were obtained at higher values, $3.25 \lesssim s_0 \leq 4 \text{ GeV}^2$, in Ref. [14], it seems reasonable to infer that $s_0 = m_\tau^2$ is too small for the OPE to reliably describe the R -ratio through the spectral integrals appearing in the FESRs (1.6) — even more so if, in addition, the OPE is naively truncated. Another possible contributor to the difference might be that the R -ratio spectral integrals, being more precise than their counterparts obtained

¹⁰ Reference [13] confirms this, even though that reference explains why this does not imply that the tOPE is a reliable strategy.

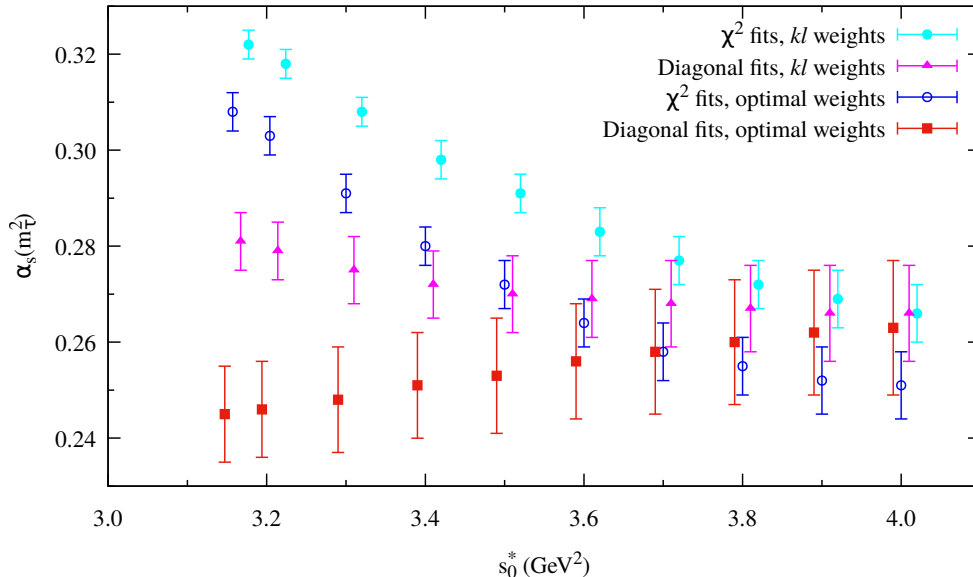


FIG. 2: $\alpha_s(m_\tau^2)$ as a function of s_0 . Blue points (open circles) are correlated optimal-weight fit results, red points (squares) are diagonal optimal-weight fit results, cyan points (filled circles) are correlated kl -spectral weights fit results, and magenta points (triangles) are diagonal kl -spectral weights fit results. Red, cyan and magenta points are slightly offset horizontally for better visibility.

from τ -decay data, provide a more stringent test of the tOPE strategy.¹¹

In order to make progress, given this somewhat inconclusive state of affairs, we proceed to consider fits of Eq. (1.6) using a value $s_0 = s_0^*$ larger than m_τ^2 . We increase s_0^* (in steps of 0.1 GeV^2 , starting from $s_0^* = 3.2 \text{ GeV}^2$) until the corresponding correlated fit produces a p -value greater than 10%. For the optimal and kl spectral weight sets, we find this occurs for $s_0^* = 3.6 \text{ GeV}^2$ and $s_0^* = 3.7 \text{ GeV}^2$, respectively. Both correlated and diagonal fit results are shown in the second lines of Tables 1 and 2, respectively. We see that the results obtained from correlated and diagonal fits are in good agreement for both set of weights. However, the correlated fit values for $\alpha_s(m_\tau^2)$ obtained from the optimal and kl spectral weight fits are around 2.5σ or more apart.¹²

We show results for the strong coupling for each of these types of fits, as a function of s_0^* , in Fig. 2, with correlated fit results for $\alpha_s(m_\tau^2)$ for optimal, respectively, kl spectral weights shown as blue, respectively, cyan points, and diagonal fit results shown as red, respectively, magenta points. We emphasize that correlated fits with s_0^* smaller than 3.6 GeV^2 have very small p -values, which rapidly deteriorate down toward $s_0^* = m_\tau^2$. In the region where

¹¹ The fact that our investigation uses only V -channel data, instead of $V + A$, is much less likely to explain the difference, given the good quality fits of the τ -based V channel data obtained in Ref. [17].

¹² Note that these two values are essentially 100% correlated.

good correlated fits can be obtained, *i.e.*, for $s_0^* \gtrsim 3.6 \text{ GeV}^2$, there is good agreement with diagonal fits for each set of weights, with the correlated fits yielding the smaller errors. However, there is less good agreement between the results obtained using the optimal and $k\ell$ spectral weight sets. If we were to attempt extracting a value of $\alpha_s(m_\tau^2)$ from this collection of fits, we would have to accept a central value of roughly 0.26–0.27, which is again very low compared to the world average; in particular, compared with the values obtained in Refs. [11, 14, 16, 17, 20, 21].

A much more stringent test of the quality of these fits, and thus the assumptions underlying the tOPE strategy, is provided by consideration of the double-differences $\Delta_w^{(2)}(s_0; s_0^*)$ defined in Eq. (2.2), which we will turn to next. As explained above, a fundamental assumption of the tOPE strategy is that it provides a good theoretical description of the data for the spectral moments $I_w^{\text{exp}}(s_0)$ above $s_0 \approx m_\tau^2$. Given a fit at some $s_0 = s_0^*$, we can vary s_0 , and plot $\Delta_w^{(2)}(s_0; s_0^*)$ as a function of s_0 . If the assumption is correct, we should find good agreement between theory (fitted at s_0^*) and experiment, for any value $s_0 \geq m_\tau^2$. This means we should find that $\Delta_w^{(2)}(s_0; s_0^*) = 0$ within errors for $m_\tau^2 \leq s_0 \leq 4 \text{ GeV}^2$ for all weights w included in the fit.

In Figs. 3 to 10 we show the data and the fitted theory curves, as well as the double differences $\Delta_w^{(2)}(s_0; s_0^*)$ for the diagonal fits at $s_0^* = m_\tau^2$ in the optimal (Figs. 3 and 4) and $k\ell$ spectral (Figs. 5 and 6) weight cases; for the correlated fit at $s_0^* = 3.6 \text{ GeV}^2$ in the optimal weight case (Figs. 7 and 8); and for the correlated fit at $s_0^* = 3.7 \text{ GeV}^2$ in the $k\ell$ spectral weight case (Figs. 9 and 10). We emphasize again that all errors shown in all five panels in all four double-difference plots have been computed taking all correlations, including those between data and the fit parameters, into account.

Figures 3, 5, 7, and 9, which show the data compared with the fitted theory curves (using central values for the fit parameters) show what the fits look like, as a function of s_0 . It is clear that the theory, fixed by a fit at $s_0 = s_0^*$, does not do a very good job of describing the s_0 dependence, but, given the strong correlations, it is hard to ascertain, from these figures alone, how bad this problem actually is. It is for this reason that we focus on the comparison between experiment and theory provided by the “double-difference” figures, where we consider the quantity $\Delta_w^{(2)}(s_0; s_0^*)$ as a function of s_0 for the fixed values of s_0^* used in the corresponding fits. These results are shown in Figs. 4, 6, 8, and 10.

Three different observations are of relevance to assessing the lessons to be learned from the results shown in the double-difference figures. First, in obtaining results from a fit at $s_0 = s_0^*$, it has been assumed that the tOPE strategy provides a valid theory representation at that value of s_0 . This implies, with certainty, that this strategy should provide a good theory representation for any value of $s_0 \geq s_0^*$. The plots of $\Delta_w^{(2)}(s_0; s_0^*)$ for $s_0 > s_0^*$ directly test this assumption. Second, if the claim is that the tOPE strategy works at $s_0 = m_\tau^2$, this implies that, for any $s_0^* \in [m_\tau^2, 4 \text{ GeV}^2]$, $\Delta_w^{(2)}(s_0; s_0^*)$ should be consistent with zero for all $s_0 \geq m_\tau^2$, irrespective of the value of s_0^* used in the fit. Finally, for a fit to five spectral moments (whether employing Eq. (1.10) or Eq. (1.11)) to be successful, $\Delta_w^{(2)}(s_0; s_0^*)$ has to be consistent with zero as a function of s_0 for each of the five weights in the set. If $\Delta_w^{(2)}(s_0; s_0^*)$ shows a significant deviation from zero for just one or two weights, this indicates a problem with the fit, and thus with the tOPE strategy.

From Figs. 3, 5, 7, and 9, we see that the fitted theory curves do agree within errors with all five of the corresponding weighted spectral integrals for s_0 in the vicinity of the tOPE fit point $s_0 = s_0^*$. This is, however, not typically the case for s_0 farther away from

s_0^* . One clearly observes, however, that, for many weights, $\Delta_w^{(2)}(s_0; s_0^*)$, shown in Figs. 4, 6, 8, and 10, is not consistent with zero for $m_\tau^2 \leq s_0 \leq 4 \text{ GeV}^2$, and that many points are, in fact, many σ away from zero. This is particularly true for the correlated fits shown in Figs. 8 and 10 in the region $3.25 \text{ GeV}^2 \leq s_0 < s_0^*$. This casts serious doubt on the validity of the tOPE strategy in the whole region we have investigated here, *i.e.*, the region between $s \approx m_\tau^2$ and $s = 4 \text{ GeV}^2$.

IV. DISCUSSION AND CONCLUSION

In this paper, we have continued our investigation of the validity of the truncated OPE (tOPE) approach to FESR analyses, an investigation of relevance, for example, to the determination of α_s from such analyses of hadronic τ -decay data. The key observation is that if the tOPE approach works at a “fit point” s_0^* near m_τ^2 , it should (a) certainly work at higher values of s_0^* , and (b) given a fit at $s_0 = s_0^*$ equal to m_τ^2 or higher, there should be good agreement between the experimental spectral moments and the theory representations employing the OPE parameter fit values at $s_0 \geq s_0^*$.

Under rather mild assumptions, tests of these two observations can be carried out using R -ratio data, for which very precise results are available up to $s = 4 \text{ GeV}^2$ [18, 27]. The two assumptions are that (i) it is sufficient to consider only EM vector-channel data (with the axial-channel data available in τ decays not being accessible through $e^+e^- \rightarrow \text{hadrons}$), and (ii) the presence of an $I = 0$ component in the R -ratio data does not change the behavior of the OPE in an essential way as far as the tOPE strategy is concerned. We discussed these two assumptions, and the reasons for expecting them to be reliable, in detail in Sec. II.

The tOPE approach makes two basic assumptions. The first is that violations of quark-hadron duality can be ignored already at energies as low as the τ mass, and the second that the expansion in $1/s_0$ of the integrated OPE, though in actual fact divergent, acts as if it were rapidly converging already at $s_0 = m_\tau^2$. If we assume that in the region $s_0 \gtrsim m_\tau^2$ duality violations are relatively unimportant (an assumption that is consistent with the results of Ref. [14]),¹³ the question centers on the nature of the OPE for values of Q^2 with $|Q^2| = s_0$ in this region.

Our central results are shown in Figs. 4, 6, 8, and 10. If the tOPE were to be valid, they should show data points consistent with zero for all $s_0 \geq m_\tau^2$. Instead, these figures show very significant disagreements, as a function of s_0 , between the experimental values of the spectral moments and the theory representations based on the tOPE fits at various fit points s_0^* , for both the optimal-weight- and $k\ell$ -spectral-weight-based fits. We emphasize that the error bars shown for the double differences, defined in Eq. (2.2), take all correlations into account, including those between data and the fit parameter values.

The first two of these figures show the results of diagonal fits at $s_0^* = m_\tau^2$, which we considered after we found that correlated fits do not work at this s_0^* (*cf.* Tables 1 and 2). More important are the fits at $s_0^* = 3.6 \text{ GeV}^2$ (for optimal weights, shown in Fig. 8) and $s_0^* = 3.7 \text{ GeV}^2$ (for $k\ell$ spectral weights, shown in Fig. 10). These are correlated χ^2 fits with acceptable p -values, where the figures nonetheless show very serious mismatches between the experimental data and the theory representations provided by the fits. We observe that

¹³ The fact that the weights (1.10) and (1.11) are doubly pinched, also serves to suppress such integrated duality violations.

if the tOPE strategy does not work for a value of s_0^* significantly larger than m_τ^2 , it certainly cannot be expected to be reliable at $s_0^* = m_\tau^2$, thus making our tests at $s_0^* = m_\tau^2$ less relevant. Nevertheless, the fact that correlated fits at $s_0^* = m_\tau^2$ do not work stands in sharp contrast to what is found with data from hadronic τ decays [13, 17].

We may also ask what our results imply for the OPE itself, rather than just for the tOPE strategy. Our tests probe the integrated OPE up to dimension 16, for both the optimal and $k\ell$ spectral weight sets. As the OPE is (at best) an asymptotic expansion, the question is to which order one can expect to be able to use it while still having the truncated expansion approach the underlying true physical value. The answer to this question will, of course, depend on the value of s_0 . The analysis in Ref. [14] showed that the OPE provides a consistent representation of the EM vacuum polarization up to dimension $D = 10$, a conclusion supported, in particular, by the consistency of the results for the effective $D = 6$ condensate, C_6 , obtained using different weights with degree up to 4, in the region $m_\tau^2 \leq s_0 \leq 4 \text{ GeV}^2$. It is possible that the OPE starts to already diverge before one reaches the term of dimension 16 for s_0 in the range between m_τ^2 and 4 GeV^2 , but it is also possible that it approaches the (unknown) exact answer reasonably well, to this order, and in this range. Our tests leave this question undecided. What they do show is that even if the OPE is still approaching the true answer out to $D = 16$, it is not doing so rapidly enough that terms with $D > 10$ (for the optimal weights) or $D > 8$ (for the $k\ell$ spectral weights) can be neglected, in the sum rules considered here. In any case, our analysis provides a clear message that it is safest to restrict the analysis to those observables which only receive a contribution from the lower-dimension terms in the OPE.

Our main conclusion is that even if one considers an energy region in which duality violations are likely to be strongly suppressed, the tOPE strategy leads to inconsistent results, thus invalidating the neglect of higher-order terms in the OPE in that energy region. Taken together with our earlier investigations of the tOPE strategy reported in Ref. [13], the implication is that the tOPE strategy is not a reliable one. It should thus no longer be employed, for example, in the extraction of α_s from hadronic τ decays or R -ratio data, up to at least $s = 4 \text{ GeV}^2$, particularly since an alternative method which does not suffer from the shortcomings of the tOPE strategy exists [11, 14, 20, 21].

Acknowledgments

DB, KM and SP would like to thank the Department of Physics and Astronomy at San Francisco State University for hospitality, and MG would like to thank the Department of Mathematics and Statistics at York University for hospitality. The work of DB is supported by the São Paulo Research Foundation (FAPESP) Grant No. 2015/20689-9 and by CNPq Grant No. 309847/2018-4. The work of MG is supported by the U.S. Department of Energy, Office of Science, Office of High Energy Physics, under Award Number DE-FG03-92ER40711. KM is supported by a grant from the Natural Sciences and Engineering Research Council of Canada. SP is supported by CICYTFEDER-FPA2017-86989-P and by Grant No. 2017 SGR 1069.

-
- [1] Y. S. Tsai, Phys. Rev. D **4**, 2821 (1971) Erratum: [Phys. Rev. D **13**, 771 (1976)].
[2] J. Erler, Rev. Mex. Fis. **50**, 200 (2004) [hep-ph/0211345].

- [3] R. Shankar, Phys. Rev. D **15**, 755 (1977); R. G. Moorhouse, M. R. Pennington and G. G. Ross, Nucl. Phys. B **124**, 285 (1977); K. G. Chetyrkin and N. V. Krasnikov, Nucl. Phys. B **119**, 174 (1977); K. G. Chetyrkin, N. V. Krasnikov and A. N. Tavkhelidze, Phys. Lett. B **76**, 83 (1978); N. V. Krasnikov, A. A. Pivovarov and N. N. Tavkhelidze, Z. Phys. C **19**, 301 (1983); E. G. Floratos, S. Narison and E. de Rafael, Nucl. Phys. B **155**, 115 (1979); R. A. Bertlmann, G. Launer and E. de Rafael, Nucl. Phys. B **250**, 61 (1985).
- [4] E. Gamiz *et al.*, JHEP, **0301**, 060 (2003); Phys. Rev. Lett., **94**, 011803 (2005); PoS, **KAON 2007**, 008 (2008).
- [5] K. Maltman, *et al.*, Nucl. Phys. Proc. Suppl., **189**, 175 (2009); K. Maltman, Nucl. Phys. Proc. Suppl., **218**, 146 (2011).
- [6] R. J. Hudspith, R. Lewis, K. Maltman and J. Zanotti, Phys. Lett. B **781**, 206 (2018) [arXiv:1702.01767 [hep-ph]].
- [7] M. Davier, L. Girlanda, A. Höcker and J. Stern, Phys. Rev. D **58**, 096014 (1998) [hep-ph/9802447]; S. Dürr and J. Kambor, Phys. Rev. D **61**, 114025 (2000) [hep-ph/9907539]; M. Golterman, K. Maltman and S. Peris, Phys. Rev. D **89**, no. 5, 054036 (2014) [arXiv:1402.1043 [hep-ph]].
- [8] E. C. Poggio, H. R. Quinn and S. Weinberg, Phys. Rev. D **13**, 1958 (1976).
- [9] K. Maltman, Phys. Lett. B **440**, 367 (1998); C. A. Dominguez and K. Schilcher, Phys. Lett. B **448**, 93 (1999).
- [10] O. Catà, M. Golterman and S. Peris, Phys. Rev. D **79**, 053002 (2009) [arXiv:0812.2285 [hep-ph]].
- [11] D. Boito, O. Catà, M. Golterman, M. Jamin, K. Maltman, J. Osborne and S. Peris, Phys. Rev. D **84**, 113006 (2011) [arXiv:1110.1127 [hep-ph]].
- [12] D. Boito, I. Caprini, M. Golterman, K. Maltman and S. Peris, Phys. Rev. D **97**, 054007 (2018) [arXiv:1711.10316 [hep-ph]].
- [13] D. Boito, M. Golterman, K. Maltman and S. Peris, Phys. Rev. D **95**, 034024 (2017) [arXiv:1611.03457 [hep-ph]].
- [14] D. Boito, M. Golterman, A. Keshavarzi, K. Maltman, D. Nomura, S. Peris and T. Teubner, Phys. Rev. D **98**, no. 7, 074030 (2018) [arXiv:1805.08176 [hep-ph]].
- [15] F. Le Diberder and A. Pich, Phys. Lett. B **289**, 165 (1992).
- [16] M. Davier, A. Höcker, B. Malaescu, C. Z. Yuan and Z. Zhang, Eur. Phys. J. C **74**, 2803 (2014) [arXiv:1312.1501 [hep-ex]].
- [17] A. Pich and A. Rodríguez-Sánchez, Phys. Rev. D **94**, 034027 (2016) [arXiv:1605.06830 [hep-ph]].
- [18] A. Keshavarzi, D. Nomura and T. Teubner, Phys. Rev. D **97**, no. 11, 114025 (2018) [arXiv:1802.02995 [hep-ph]].
- [19] D. Boito, M. Golterman, K. Maltman and S. Peris, SciPost Phys. Proc. **1**, 053 (2019) [arXiv:1811.01581 [hep-ph]].
- [20] D. Boito, M. Golterman, M. Jamin, A. Mahdavi, K. Maltman, J. Osborne and S. Peris, Phys. Rev. D **85**, 093015 (2012) [arXiv:1203.3146 [hep-ph]].
- [21] D. Boito, M. Golterman, K. Maltman, J. Osborne and S. Peris, Phys. Rev. D **91**, 034003 (2015) [arXiv:1410.3528 [hep-ph]].
- [22] A. A. Pivovarov, Z. Phys. C **53**, 461 (1992) [Sov. J. Nucl. Phys. **54**, 676 (1991)] [Yad. Fiz. **54** (1991) 1114] [arXiv:hep-ph/0302003]; F. Le Diberder and A. Pich, Phys. Lett. B **286**, 147 (1992).
- [23] M. Beneke and M. Jamin, JHEP **0809**, 044 (2008) [arXiv:0806.3156 [hep-ph]].

- [24] M. Beneke, D. Boito and M. Jamin, JHEP **1301**, 125 (2013) [arXiv:1210.8038 [hep-ph]].
- [25] M. Tanabashi *et al.* [Particle Data Group], Phys. Rev. D **98**, no. 3, 030001 (2018).
- [26] G. P. Salam, arXiv:1712.05165 [hep-ph].
- [27] M. Davier, A. Höcker, B. Malaescu and Z. Zhang, Eur. Phys. J. C **77**, no. 12, 827 (2017) [arXiv:1706.09436 [hep-ph]].

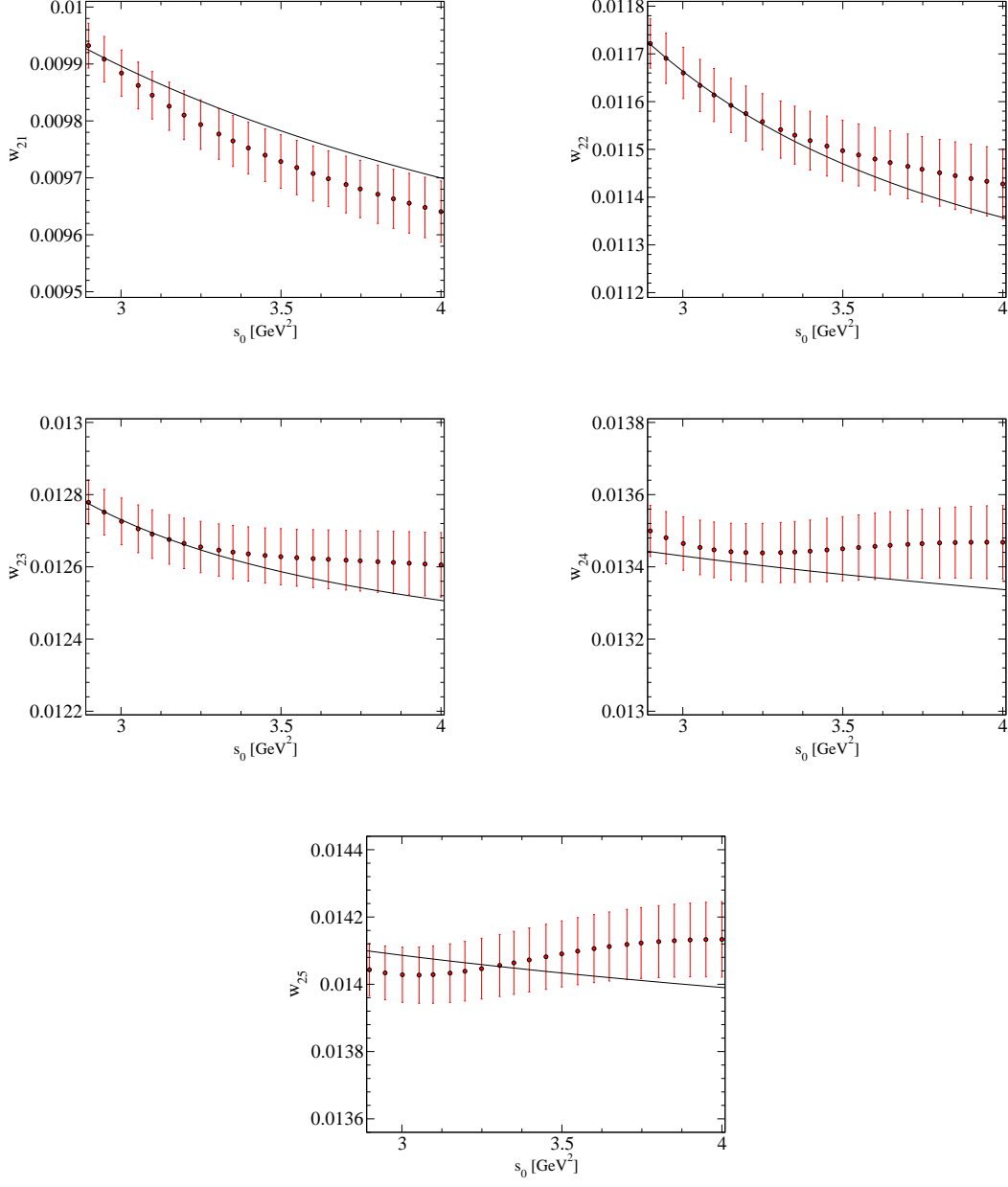


FIG. 3: Comparison of $I_w^{\text{exp}}(s_0)$ with $I_w^{\text{th}}(s_0)$ with parameter values obtained from diagonal fits with optimal weights, as a function of s_0 with $s_0^* = m_\tau^2$.

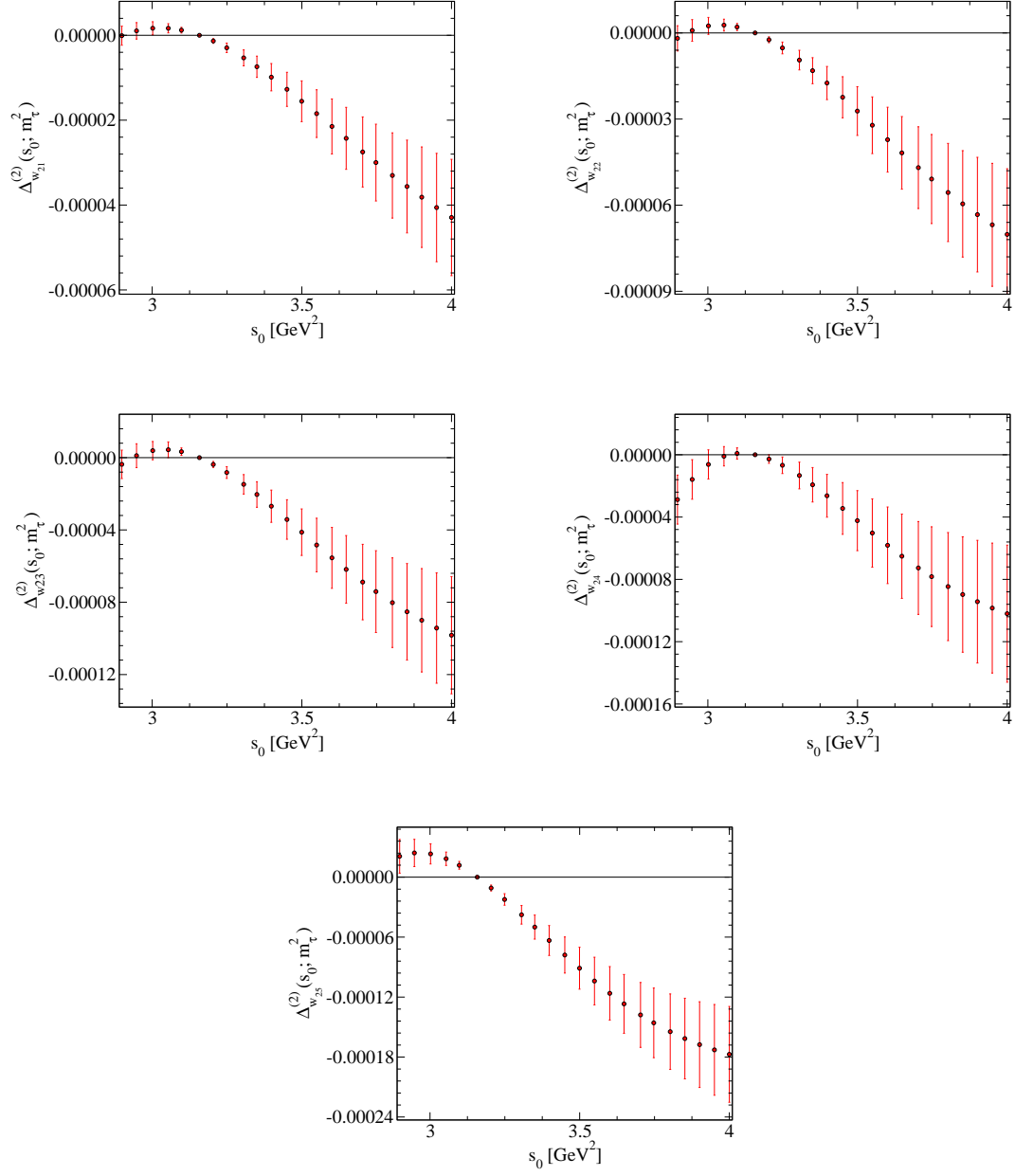


FIG. 4: The double differences, $\Delta_w^{(2)}(s_0; s_0^*)$, obtained from diagonal fits with optimal weights, as a function of s_0 with $s_0^* = m_\tau^2$.

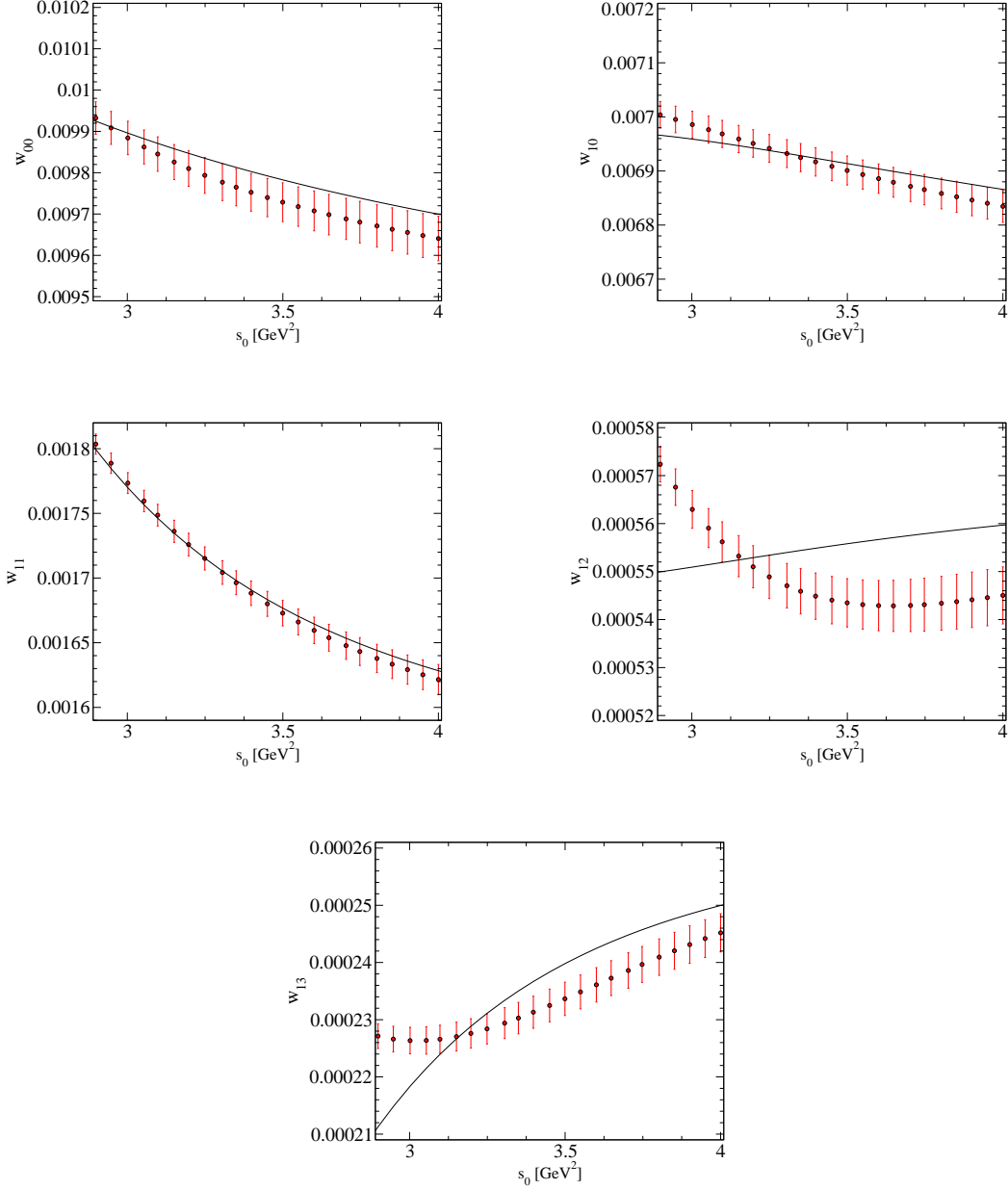


FIG. 5: Comparison of $I_w^{\text{exp}}(s_0)$ with $I_w^{\text{th}}(s_0)$ with parameter values obtained from diagonal fits with kl spectral weights, as a function of s_0 with $s_0^* = m_\tau^2$.

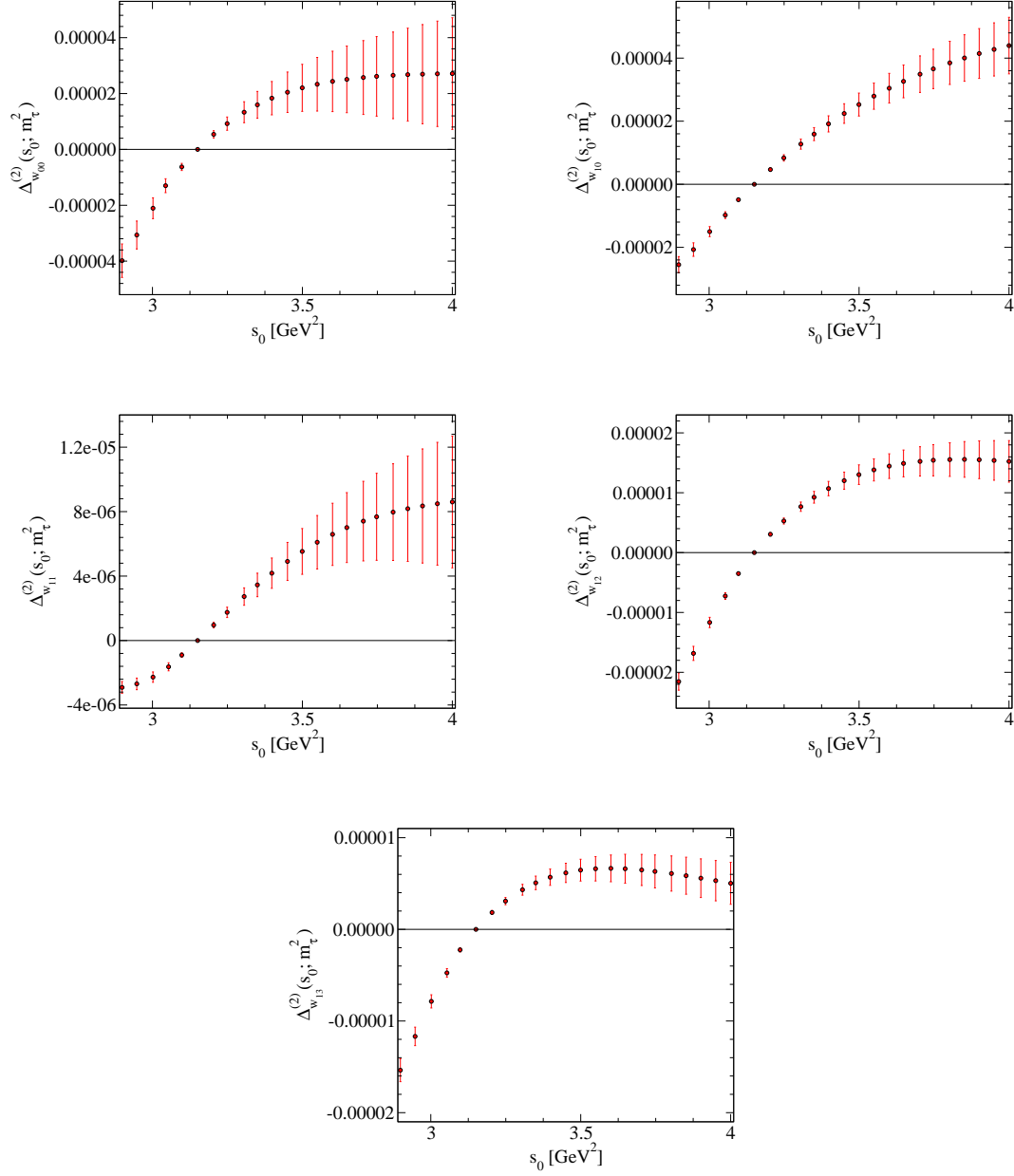


FIG. 6: The double differences, $\Delta_w^{(2)}(s_0; s_0^*)$, obtained from diagonal fits with $k\ell$ spectral weights, as a function of s_0 with $s_0^* = m_\tau^2$.

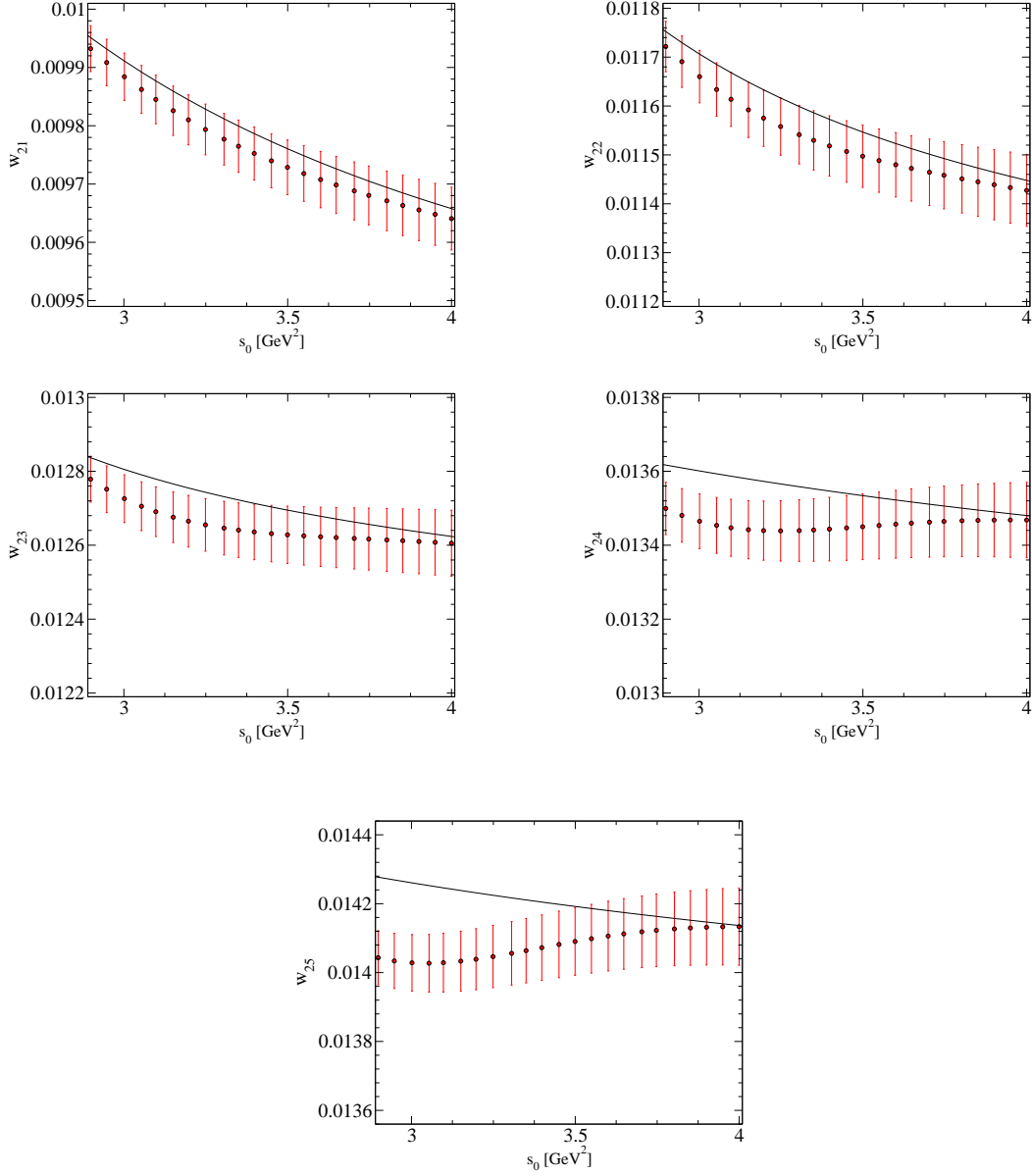


FIG. 7: Comparison of $I_w^{\text{exp}}(s_0)$ with $I_w^{\text{th}}(s_0)$ with parameter values obtained from correlated fits with optimal weights, as a function of s_0 with $s_0^* = 3.6 \text{ GeV}^2$.

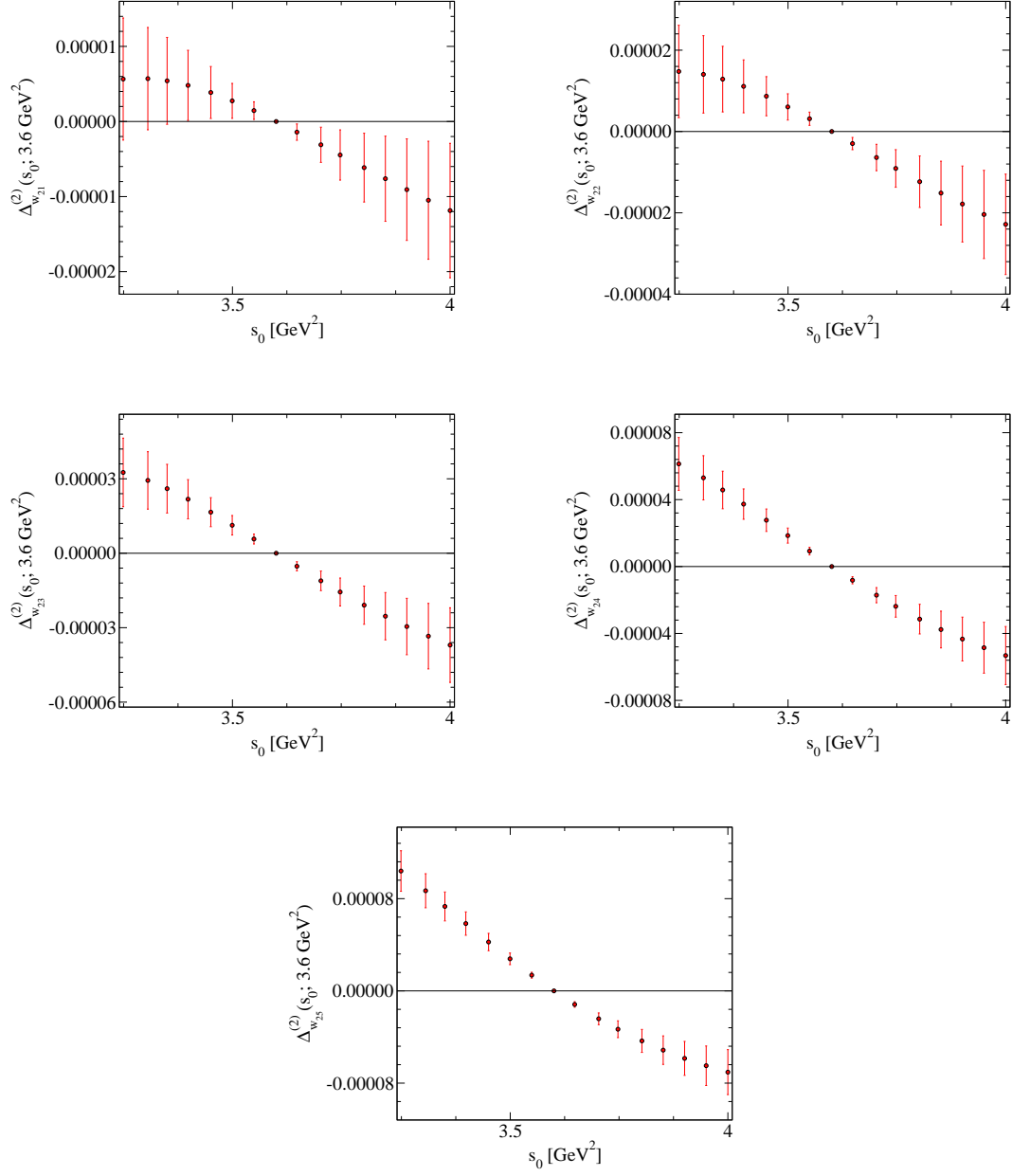


FIG. 8: The double differences, $\Delta_w^{(2)}(s_0; s_0^*)$, obtained from correlated fits with optimal weights, as a function of s_0 with $s_0^* = 3.6 \text{ GeV}^2$.

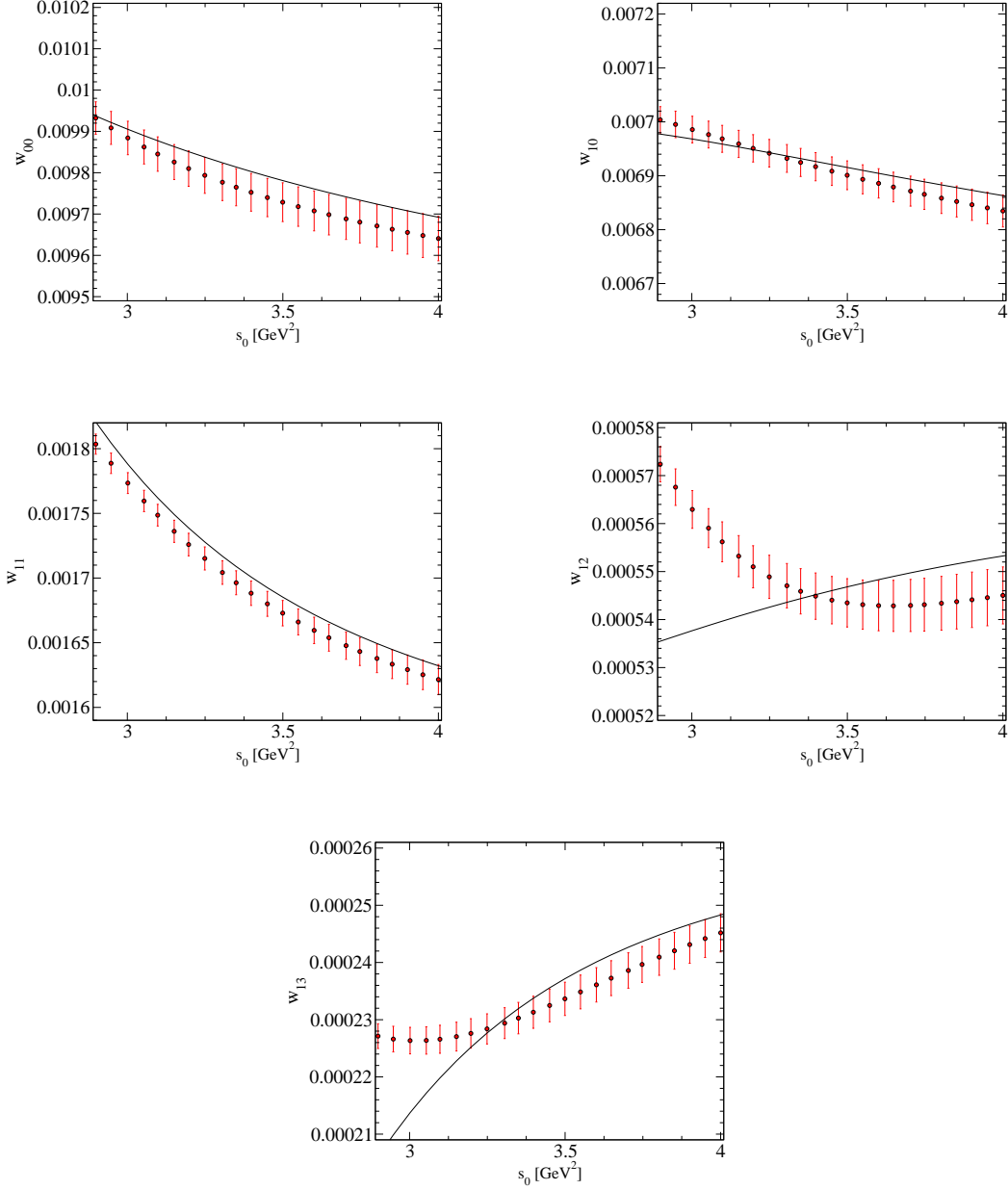


FIG. 9: Comparison of $I_w^{\text{exp}}(s_0)$ with $I_w^{\text{th}}(s_0)$ with parameter values obtained from correlated fits with kl spectral weights, as a function of s_0 with $s_0^* = 3.7$ GeV².

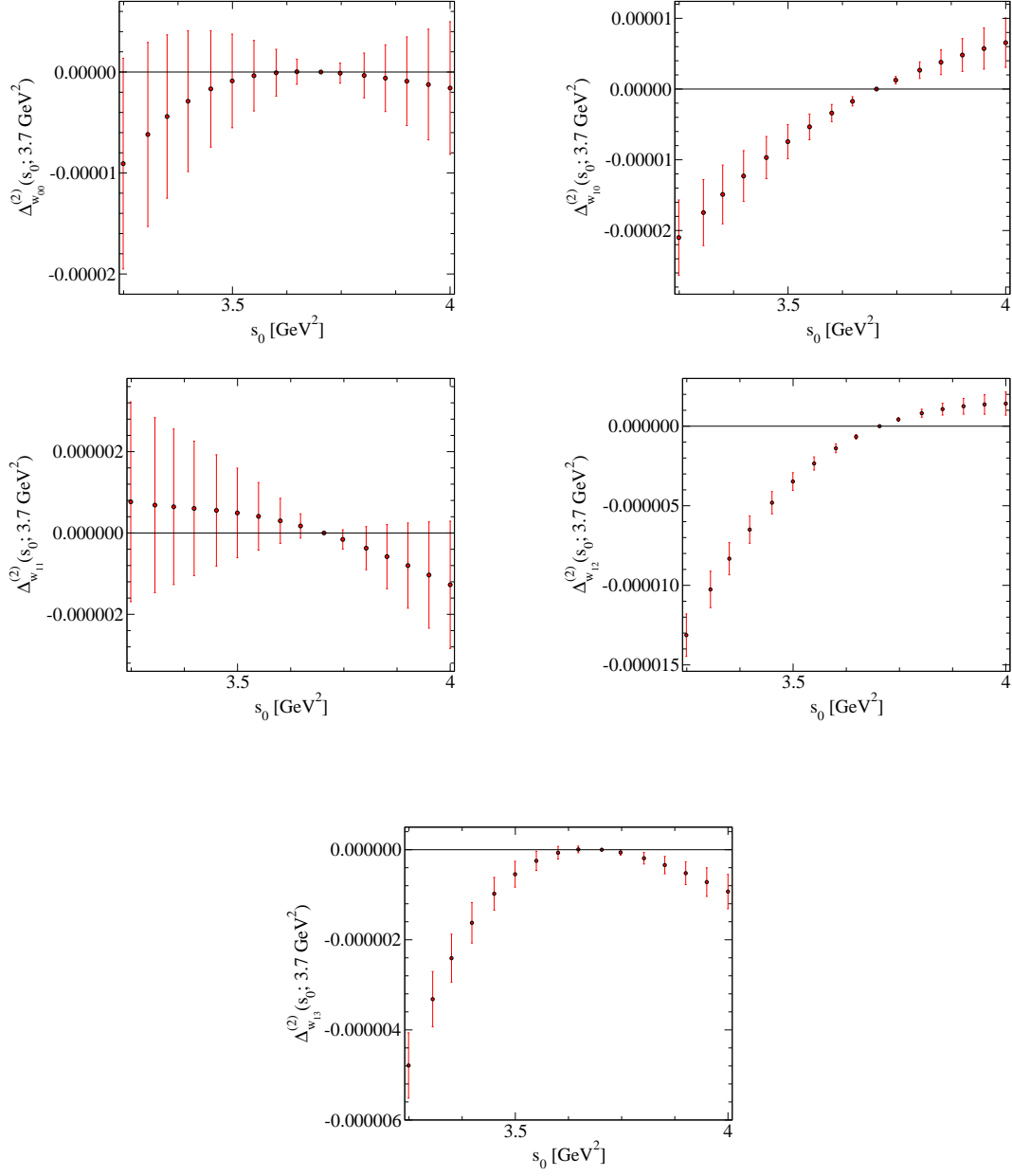


FIG. 10: The double differences, $\Delta_w^{(2)}(s_0; s_0^*)$, obtained from correlated fits with $k\ell$ spectral weights, as a function of s_0 with $s_0^* = 3.7 \text{ GeV}^2$.